



Development and investigation of mixed-matrix PVA-fullerenol membranes for acetic acid dehydration by pervaporation



Maria E. Dmitrenko^a, Anastasia V. Penkova^{a,*}, Alexander B. Missyul^b, Anna I. Kuzminova^a, Denis A. Markelov^{a,c}, Sergey S. Ermakov^a, Denis Roizard^d

^a St. Petersburg State University, 7/9 Universitetskaya nab., St. Petersburg 199034, Russia

^b ALBA Synchrotron Light Source, Carrer de la Llum 2-26, 08290 Cerdanyola del Vallès, Barcelona, Spain

^c St. Petersburg National Research University of Information Technologies, Mechanics and Optics, Kronverkskiy pr. 49, 197101 St. Petersburg, Russia

^d Laboratoire Réactions et Génie des Procédés, CNRS, Université de Lorraine, ENSIC, 1 rue Granville, 54000 Nancy, France

ARTICLE INFO

Article history:

Received 11 April 2017

Received in revised form 22 June 2017

Accepted 22 June 2017

Available online 23 June 2017

Keywords:

Acetic acid

Dehydration

Polyvinyl alcohol

Fullerenol

Membrane

Pervaporation

ABSTRACT

This study focuses on the development of a green pervaporation (PV) process for dehydrating a wide range of commercially significant mixtures such as concentrated (and corrosive) acetic acid blends using mixed-matrix membranes based on polyvinyl alcohol (PVA) cross-linked by low-hydroxylated fullerenol (C₆₀(OH)₁₂). The effect of C₆₀(OH)₁₂ and various conditions of physical cross-linking on the structure and internal morphology of composite membranes was investigated by X-ray diffraction and scanning electron microscopy, and the stability and transport properties of the developed membranes were investigated for acetic acid dehydration at a wide range of feed water contents (5–30 wt.%) and temperatures (25–60 °C). The supported mixed-matrix membranes exhibited high permeances and water selectivities, as well as good stability toward feed mixtures, with the best transport properties obtained for a C₆₀(OH)₁₂(5 wt.%)–PVA supported composite membrane thermally treated at 140 °C for 420 min.

© 2017 Elsevier B.V. All rights reserved.

1. Introduction

Dehydration is an important process in chemical industry, used either to avoid side reactions and catalyst poisoning or to achieve enhanced post-synthesis purification, with more than 3000 studies on dehydration currently reported. Notably, dehydration is a complicated process, since many industrially important alcohols (e.g., ethanol, propanol, and butanol), organic solvents (e.g., tetrahydrofuran, acrolein, dichloromethane, and hexane), and acids (e.g., acetic acid and formic acid) exhibit low volatility and strong affinity to water. The above properties can lead to the formation of azeotropes [1,2], hindering the separation of water by distillation, which is the most common dehydration technique. Azeotrope breaking can be realized by utilizing a hybrid process that combines distillation and pervaporation, presenting a technically and economically attractive solution that is less expensive than distillation under reduced pressure or dehydration by molecular sieves [3,4].

According to global organic acid production data [5], acetic acid (AcOH; both dilute and glacial) is the most widely industrially used acid (annual global production = 13 million ton), particularly for the manufacture of chemicals, being one of the top 20 organic intermediates used in chemical industry. Acetic acid is mainly used as a reagent for producing compounds such as cellulose acetate, vinyl plastics, latex paints, and textile finishes, being additionally required as a solvent and an intermediate [6–9]. Although water and acetic acid do not form an azeotrope, the separation of their mixtures by traditional distillation requires a large number of trays in the distillation column and a high reflux ratio, making this procedure energy-expensive because of the small volatility differences between water and AcOH [10]. Pervaporation is a potentially useful method for separating AcOH/water mixtures [11–13], offering numerous advantages over existing processes, such as high selectivity for water, low energy consumption for separation of azeotropic mixtures and close-boiling components, and modular and compact installation using spiral or hollow fiber modules [14]. Moreover, pervaporation is an environmental friendly process, not requiring the addition of volatile components. However, it should be noted that at high AcOH concentration, the AcOH/water mixture is highly corrosive and may alter membrane properties during dehydration. Therefore, the development of chemically

* Corresponding author.

E-mail addresses: m.dmitrienko@spbu.ru (M.E. Dmitrenko), a.penkova@spbu.ru (A.V. Penkova), amissiu@cells.es (A.B. Missyul), ai.kuzminova@mail.ru (A.I. Kuzminova), markeloved@gmail.com (D.A. Markelov), s.ermakov@spbu.ru (S.S. Ermakov), denis.roizard@univ-lorraine.fr (D. Roizard).

resistant polymeric membranes for acid dehydration is highly relevant.

This study focuses on the development of green polymeric membranes that are stable in strongly acidic media and exhibit high separation performance. Some polymeric membranes for organic acid dehydration are commercially available, as exemplified by polyvinyl alcohol (PVA)-based PERVAP membranes for AcOH/water separation developed by Sulzer Chemtech (Switzerland). Moreover, it should be noted that the Energy Research Centre of the Netherlands (ECN, the Netherlands) reported a new tubular inorganic HybSi[®]-AR membrane in 2016, which is resistant to organic acids even at very low pH values and is suited for high-temperature use [15]. Among the above membranes, nanocomposite polymeric membranes, combining the properties of organic and inorganic particles, are considered most promising.

Currently, no membranes for organic acid dehydration exhibiting excellent transport properties exist. Hence, a lot of research effort is directed at improving the properties of membrane materials. Material engineering mostly focuses on improving the properties of well-known hydrophilic materials such as polyvinyl alcohol, chitosan [16], alginate [17], polyimide, polyphenylsulfone [18], cellulose esters (e.g., by fabricating mixed-matrix membranes based on polymers with different inorganic and organic particles [16]: polyelectrolyte complexes [19], and inorganic materials such as silica and zeolites [18,20]). A previous review [16] summarizes the main research progress achieved in hydrophilic pervaporation up to 2007, focusing on the dehydration of AcOH/water mixtures by pervaporation through various membranes with different types of cross-linkers and modification methods, e.g., those based on PVA, Nafion, NaAlG, polycarbonate, tetrahydroxysilane (TEOS), acrylonitrile/maleic anhydride, and zeolites.

Based on the above reports, we developed a new series of composite supported membranes, using PVA and fullereneol (C₆₀(OH)₁₂) nanoparticles for cross-linking and promoting their selectivity for water [21–23]. The use of functionalized fullerene allowed the formation of ether cross-linkages to further improve the chemical resistance of membranes in acidic feed mixtures.

Herein, we focused on developing and improving the following aspects:

- Cross-linking utilizing PVA and fullereneol by heat treatment at 140 °C of variable duration (100–420 min).
- Formation of novel supported membranes with thin PVA and PVA-fullereneol cross-linked active layers coated on a UPM porous support to simultaneously achieve high water selectivity and high permeance required for industrial applications.

Additionally, it was foreseen that the use of a selective layer based on water-soluble components such as PVA and fullereneol in supported membranes might afford “greener” membranes that could be used to design energy-efficient processes for the dehydration of acetic acid.

2. Materials and methods

2.1. Materials

PVA with a molecular weight of 141 kDa purchased from ZAO LenReaktiv (certificate of analysis No. 553041-3013, date of manufacture 09.2011) was used as the membrane material, and C₆₀(OH)₁₂ (Fullerene Technologies, Russia) was used for PVA modification. A hydrophilic porous membrane based on aromatic polysulfone amide (UPM, pore size 200 Å) was purchased from Vladipor (Russia) and used as a membrane support. Acetic acid was purchased from Sigma-Aldrich (France).

2.2. Membrane preparation

2.2.1. Dense membranes

PVA composite membranes were prepared according to a previously reported procedure [21]: the composite membranes (thickness 40 ± 2 μm) with the desired quantity of fullereneol (0–5% w/w with respect to the weight of the polymer) were prepared by using a solution casting method and dried by solvent evaporation at 40 °C for 24 h. Then, the obtained polymer membranes were cross-linked by thermal treatment at 140 °C during different time (100, 120, 180, 240, 300, 360 and 420 min). Above the optimal cross-linking temperature of 140 °C, fullereneol molecules exhibited decomposition due to OH group loss.

2.2.2. Supported membranes

The thin selective layer of supported membranes was produced by casting a 2 wt.% aqueous solution of PVA without and with fullereneol (1 and 5 wt.% with respect to polymer) onto the surface of the UPM support and drying at room temperature. The fabricated layer had a thickness of 1.5 ± 0.3 μm, as determined by scanning electron microscopy (SEM) measurements, and its cross-linking was achieved by heating the membrane at 140 °C for various times (100, 240, and 420 min), making use of the optimized results obtained for dense membranes.

The maximum loading of fullereneol was limited to 5 wt.%, with higher concentrations leading to poor dispersion in membranes and causing defects and inferior mechanical properties. The preparation conditions and names of the thus fabricated membranes are listed in Table 1.

2.3. Sorption experiments

In gravimetric sorption experiments, membrane films of known weight were immersed in a liquid at 20 °C. Three days later, the excess liquid was removed, and the membranes were weighed. This procedure was repeated until the weight of the swollen films remained constant. The degree of equilibrium swelling or liquid sorption of the polymer membrane, *S* (g liquid/100 g dry polymer), was calculated as:

$$S = (m_S - m_0)/m_0, \quad (1)$$

where *m_S* is the weight of the swollen membrane, and *m₀* is the weight of the dry membrane.

Table 1
Prepared PVA membrane samples.

Membrane name	Type	Thickness of dense layer (μm)	Heat treatment time (min)/fullereneol loading (wt.%)
PVA-100	Dense	40	100/0
PVA-100 ^{sup}	Supported	1.5	100/0
PVA-1 ^a -100	Dense	40	100/1
PVA-1 ^a -100 ^{sup}	Supported	1.5	100/1
PVA-5 ^a -100	Dense	40	100/5
PVA-5 ^a -100 ^{sup}	Supported	1.5	100/5
PVA-240	Dense	40	240/0
PVA-240 ^{sup}	Supported	1.5	240/0
PVA-1 ^a -240	Dense	40	240/1
PVA-5 ^a -240	Dense	40	240/5
PVA-420	Dense	40	420/0
PVA-420 ^{sup}	Supported	1.5	420/0
PVA-1 ^a -420	Dense	40	420/1
PVA-1 ^a -420 ^{sup}	Supported	1.5	420/1
PVA-5 ^a -420	Dense	40	420/5
PVA-5 ^a -420 ^{sup}	Supported	1.5	420/5

^a To simplify membrane naming, “1” and “5” correspond to fullereneol loading in wt.%.

2.4. Wide-angle X-ray diffraction

The X-ray diffraction (XRD) patterns of investigated membranes were recorded at room temperature using a Bruker D8 DISCOVER diffractometer (Cu K_{α} radiation, 40 kV, 40 mA, step size = 0.05°, scan rate = 5 s/step) for $2\theta = 5\text{--}70^\circ$ in the Bragg-Brentano geometry. Rietveld refinement was performed using the GSAS package [24] with EXPGUI interface [25], and peak shape was described by the pseudo-Voigt function.

2.5. SEM characterization

Dense and supported membranes were submerged in liquid nitrogen for 5 min and fractured perpendicularly to the surface. The prepared specimens were imaged using a scanning electron microscope (Zeiss Merlin) at a voltage of 1 kV.

2.6. Contact angle determination

Changes of surface hydrophilicity/hydrophobicity were investigated by measuring the contact angles of polymer membranes with water droplets. These measurements utilized the sessile drop method and a device named “Contact angle and surface tension meter revision 1.31.”

2.7. Pervaporation experiments

Transport properties were studied using a laboratory cell in steady state regime at 25–60 °C (Fig. 1).

A downstream pressure of $<10^{-2}$ kPa was maintained using a vacuum pump, being controlled by a pressure gauge. The permeate was collected in a liquid-nitrogen-cooled trap, weighed, and analyzed by gas chromatography. The utilized gas chromatograph (SHIMADZU GC-2010) was equipped with an HP-PLOT/U column and a thermal conductivity detector to perform quantitative analysis of the feed/permeate. The concentration of feed mixtures during pervaporation was kept always constant to carry out pervaporation process at the same conditions to avoid the nonreproducibility of the transport parameters during the separation of the same feed mixture. The average stage cut was below 5%.

The membrane permeation flux, J ($\text{kg}/\text{m}^2 \text{ h}$), was determined as the amount of liquid transported through a unit membrane area per hour (Eq. (2)):

$$J = \frac{W}{A \times t}, \quad (2)$$

where W (kg) is the weight of liquids that permeated the membrane, A (m^2) is the effective membrane area, and t (h) is the measurement time.

The effectiveness of pervaporation-based binary mixture separation can be expressed by the separation coefficient β (Eq. (3)) and the process separation index (PSI; Eq. (4)) [26]:

$$\beta = \frac{Y_i/(1 - Y_i)}{X_i/(1 - X_i)} \quad (3)$$

$$\text{PSI} = J \times (\beta - 1) \quad (4)$$

where Y_i and X_i are mass fractions of the favored compound i in the permeate and in the feed, respectively. PSI ($\text{kg}/(\text{m}^2 \text{ h})$) is a quantity commonly used to compare pervaporation performances of various membranes with different separation and transport properties.

Each measurement was performed at least three times, and average values were recorded for later analysis. The following mean accuracies were determined for transport parameters. Dense membranes: $\pm 0.5\%$ for selectivity, $\pm 8\%$ for flux; supported membranes: $\pm 0.2\%$ for selectivity and $\pm 5\%$ for flux.

3. Results and discussion

The transport characteristics of thermally cross-linked dense and supported PVA membranes and those of their composites with low-hydroxylated fullerene were studied for the separation of water/AcOH feed mixtures by pervaporation. Two membrane types were used: $\sim 40\text{-}\mu\text{m}$ -thick dense membranes (to accurately capture the transport properties of pristine PVA and PVA-fullerene mixed-matrix membranes) and supported membranes (with a thin selective layer $\sim 1.5\ \mu\text{m}$ thick), with the demonstrating the possibility of producing industrially interesting high-permeance membranes. Finally, an in-depth stability test of PVA-5-420^{sup} membrane in close-to-industrial conditions investigated the performance of PVA-fullerene mixed-matrix membranes at feed water contents of 10–30 wt.%.

3.1. Stability and sorption

Cross-linking conditions were further optimized based on the results of our previous studies, i.e., 100-min thermal cross-linking of PVA and PVA-fullerene membranes at 140 °C [22,23]. Membranes highly selective for water and resistant to aggressive mixtures (especially AcOH/water mixtures) were obtained by increasing the heating time from 100 to 420 min to achieve more extensive PVA cross-linking.

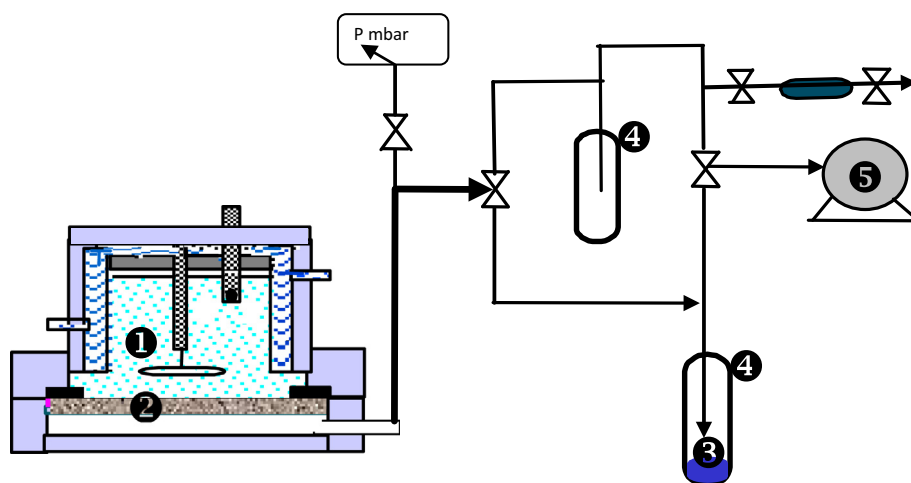


Fig. 1. Experimental pervaporation set-up (1 thermostat and water batch – 2 membrane – 3 permeate – 4 cold trap – 5 vacuum pump – atmospheric pressure).

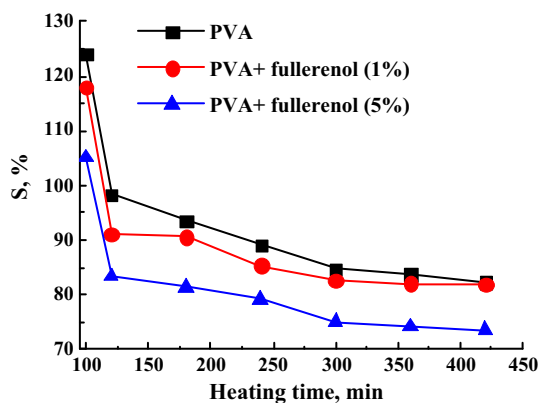


Fig. 2. Dependence of sorption degree on cross-linking heating time.

Table 2

Pervaporation of an AcOH/water mixture (10 wt.% water, 90 wt.% AcOH) at 40 °C using dense membranes.

Membranes (140 °C, 100 min)	Flux (kg/(m ² h))	Water content in permeate (wt.%)	PSI (kg/(m ² h))
PVA-100	0.023	89.6	1.76
PVA-1-100	0.021	92.0	2.15
PVA-5-100	0.020	93.9	2.89

The equilibrium swelling of dense polymer membranes was studied to (i) determine the sorption characteristics for components of the separated mixture and explain the mechanism of penetrant transport through the membrane and (ii) determine the degree of polymer chain cross-linking and increase the extent of thermal cross-linking to enhance membrane selectivity for pervaporation-based separation of AcOH/water mixtures. Fig. 2 shows the results obtained for PVA and PVA-fullereneol membranes thermally cross-linked at 140 °C for 100, 120, 180, 240, 300, 360, and 420 min.

Differences in the sorption properties of polymer membranes directly affect their transport properties. As shown in Fig. 2, the degree of dense membrane swelling in water decreased with increasing fullereneol loading and heating time. Expectedly, the effect of heating time on cross-linking was not linear, with major swelling reduction occurring after ~120 min. Interestingly, membranes containing fullereneol (even at a low loading of 1 wt.%) exhibited a larger swelling decrease. The sorption of pure acetic acid was found to be very low for all membranes, equaling ~2 wt.% and showing that water was the active agent responsible for membrane swelling. Further, we studied membranes heated for 100, 240, and 420 min to identify the temperature dependence of transport properties for the separation of AcOH/water mixtures by pervaporation. In our previous works [22,23], we revealed that membranes heated for 100 min could potentially be used to separate industrially important mixtures, with changes of membrane sorption characteristics significantly reduced after 240 min of

heating. After heating for more than 420 min, the swelling degree remained unchanged, indicating full polymer chain cross-linking.

3.2. Pervaporation through dense and supported membranes based on PVA and PVA-fullereneol composites thermally treated at 140 °C for 100 min

The transport characteristics of dense and supported membranes based on PVA and PVA-fullereneol composites thermally cross-linked at 140 °C for 100 min were determined in the pervaporation of an acetic acid/water mixture (10 wt.% water, 90 wt.% AcOH) at 40 °C, with the obtained results presented in Table 2.

The transport properties were first determined for ~40- μ m-thick dense membranes, revealing that increasing fullereneol content decreased the flux through these membranes and increased their selectivity. Fullereneol-containing PVA membranes exhibited up to 4% higher selectivities than those containing pristine PVA, exhibiting fluxes that were only 10% lower and thus showing promise for further application in acetic acid dehydration. To obtain membranes with higher permeances, supported membranes with a thin selective layer (<1.8 μ m) were successfully prepared, allowing high-performance industrial-scale pervaporation (Fig. 3).

The above mixed-matrix supported membranes comprised a thin selective layer deposited onto a porous ultrafiltration support based on aromatic polysulfone amide (UPM), which provided good mechanical strength and did not limit the downstream mass transport (Fig. 3). Fig. 4 shows a cross-section of the supported PVA-5-100^{sup} membrane, revealing the uniform structure of the dense PVA-fullereneol top layer and demonstrating the excellent adhesion of this top layer to the spongy porous support. SEM imaging found no indication of PVA penetration into pores and determined the top layer thickness as $\sim 1.5 \pm 0.3 \mu$ m. Notably, a similar SEM image was obtained for the PVA-100^{sup} membrane (not shown here).

The transport properties of supported membranes were subsequently characterized in pervaporation-based dehydration of an AcOH/water mixture (10 wt.% water, 90 wt.% AcOH) at 40 °C, with the obtained results presented in Table 3.

Introduction of fullereneol preserved the selectivity trend observed for dense membranes, with higher loadings increasing the permeate water content (by up to 3%). In addition, the low thickness of the supported membranes expectedly gave rise to high permeance, increasing the flux 6–9-fold (Tables 2 and 3). However, for a thickness decrease from 40 to 1.5 μ m, the flux increase was less pronounced than expected, which could be explained by a combination of several phenomena, e.g., more extensive cross-linking of the thin dense layer could be achieved at the same heating temperature. Moreover, the selectivity of all supported membranes decreased by ~6%, probably due to the significantly increased water flux. Nevertheless, this series of supported membranes achieved promising PSI values (Table 3; calculated using Eq. (4)) [26]. The PSI decrease with the rise fullereneol content in PVA membranes occurs due to the flux fall because of the cross-linking between the PVA and fullereneol. To increase the PSI the

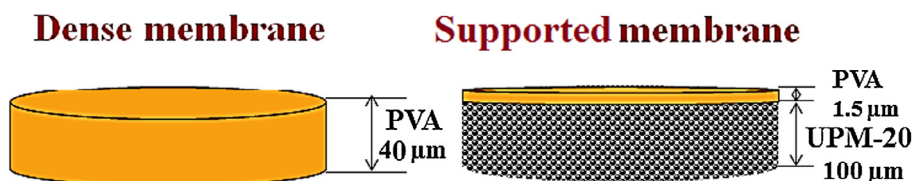


Fig. 3. Schematic structures of dense and supported membranes.

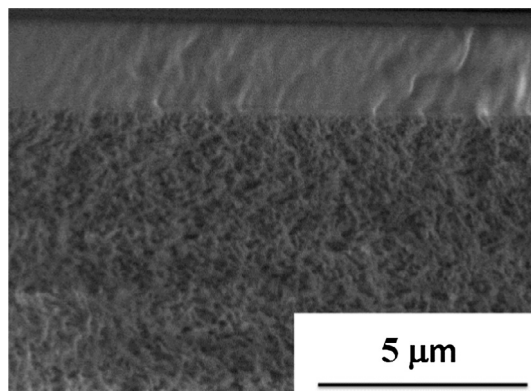


Fig. 4. Cross-sectional SEM micrograph of the PVA-5-100^{sup} membrane showing the dense PVA layer covering the surface of the porous UPM support.

Table 3

Pervaporation of an AcOH/water mixture (10 wt.% water, 90 wt.% AcOH) at 40 °C using supported membranes.

Membranes (140 °C, 100 min)	Flux (kg/(m ² h))	Water content in permeate (wt.%)	PSI (kg/(m ² h))
PVA-100 ^{sup}	0.180	83.5	8.02
PVA-1-100 ^{sup}	0.162	84.3	7.67
PVA-5-100 ^{sup}	0.112	86.6	6.40

effects of cross-linking at higher temperatures were further investigated to develop another series of supported membranes with higher selectivities and fluxes.

3.3. XRD data

The obtained XRD results corresponded to the well-known crystal structure of PVA [27] (Fig. 5). However, preliminary Pawley fitting of the obtained data showed that the crystalline domains of these samples exhibited a certain preferred orientation, as reflected by the much higher intensity of the $\bar{1}01$ peak compared

to that of the 101 peak. The layered structure of PVA, with layers parallel to the $[\bar{1}01]$ plane, is presented in Fig. 5, being different from the more common fiber-like orientation along the b axis [28], which would not change the abovementioned peak intensity ratio.

Taking into account this observation, Rietveld refinement of the obtained data was performed using the March-Dollase model [29] to describe the preferred orientation. Since the above texture implies platelet-like crystallite shape, the possibility of anisotropic peak broadening in the same direction was taken into account.

The amorphous polymer content was determined as the intensity ratio of the amorphous halo and crystalline phase peaks in the 2θ range of 12.5–30° (corresponding to 001, $\bar{1}01$, 101, and 002 peaks). Peak fitting was performed with Fityk software [30].

The results of XRD analyses are summarized in Table 4. Even though the parameter variation was close to the precision limit of laboratory XRD analysis, it could be concluded that both the overall crystallinity and the thickness of crystallites increased after heat treatment, with addition of fullereneol additionally enhancing crystallinity. This trend correlates with the observed variation of membrane pervaporation characteristics, suggesting that the crystalline polymer part plays an important role in determining these properties. In the future, a larger range of membranes should be investigated to test this hypothesis, in addition to the acquisition of higher-quality (synchrotron) diffraction data.

3.4. SEM analysis

SEM was employed for visualizing the inner morphology of membranes, with the corresponding cross-sectional micrographs of membranes based on PVA and PVA-fullereneol composites presented in Fig. 6.

Cross-sectional SEM imaging revealed that the degree of roughness significantly increased with increasing fullereneol content and heating time (Fig. 6), indicating reduced membrane flexibility and being in agreement with XRD data, which states that the degree of crystallinity for heat-treated membranes increases with increasing fullereneol concentration and heating time. SEM imaging of

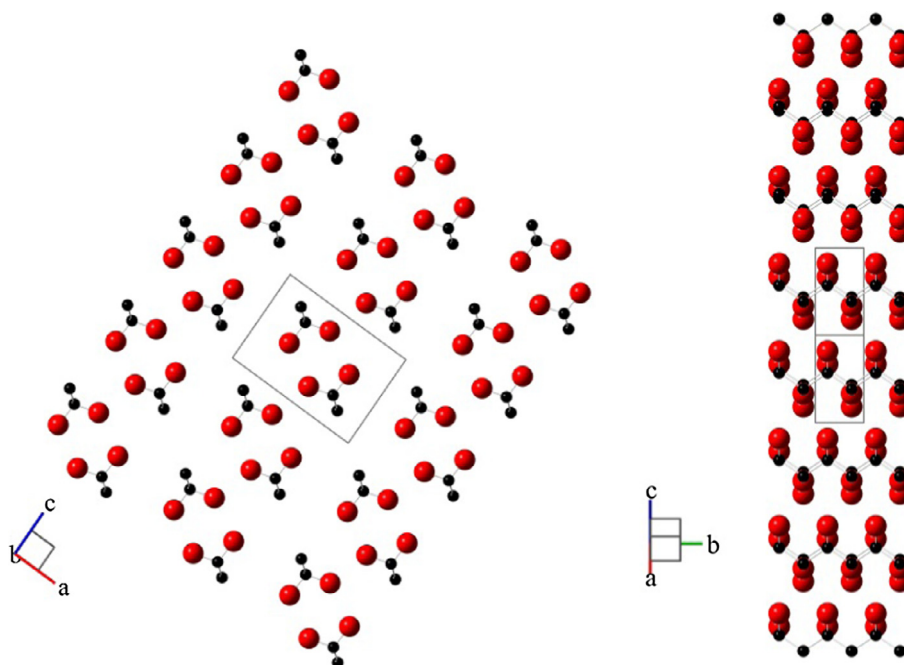


Fig. 5. Crystal structure of PVA viewed along and perpendicular to the b direction. The $[\bar{1}01]$ plane is oriented horizontally.

Table 4
Results of XRD analyses.

Sample	<i>a</i> (Å)	<i>b</i> (Å)	<i>c</i> (Å)	β (°)	R_{MD}	S size of crystallites (nm)	Size perpendicular to [1 0 1] (nm)	Crystallinity (%)
PVA-100	7.81(1)	2.534(6)	5.515(5)	91.2(1)	0.508(3)		6.5(1)	58.3
PVA-240	7.818(8)	2.541(5)	5.508(6)	90.9(1)	0.480(4)		7.9(3)	63.5
PVA-420	7.813(8)	2.552(5)	5.494(6)	90.9(1)	0.479(5)		8.2(4)	61.2
PVA-1-420	7.804(8)	2.544(6)	5.502(3)	90.9(1)	0.479(2)		8.1(1)	61.9
PVA-5-420	7.806(7)	2.538(4)	5.496(5)	90.8(1)	0.485(4)		8.5(3)	70.1

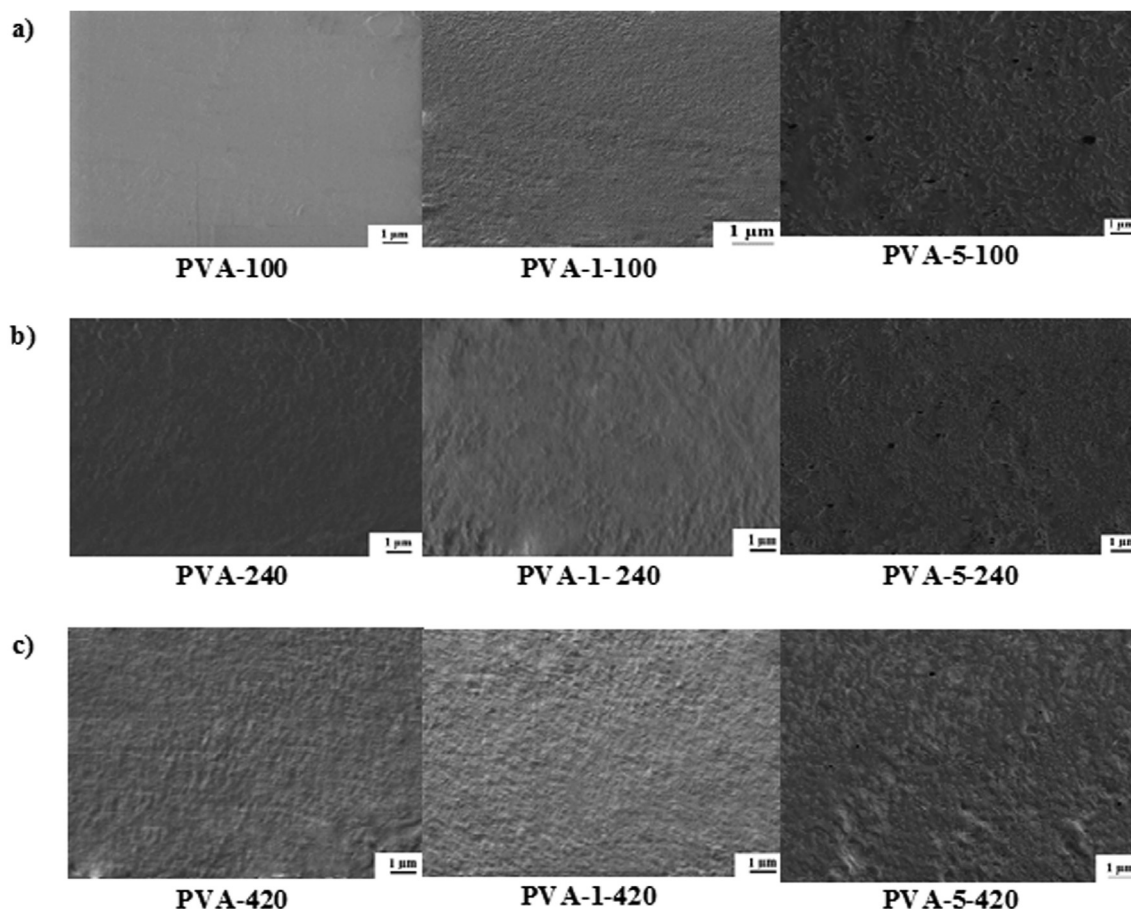


Fig. 6. Cross-sectional SEM micrographs of membranes based on PVA and PVA-fullerenol composites heated at 140 °C for 100 (a), 240 (b), 420 (c) min.

fullerenol-free membranes was conducted and discussed in our previous work [21].

3.5. Contact angle measurements

Contact angle measurements were performed using the static sessile drop method to study the changes in surface membrane morphology, with results presented in Table 5. Water is the best standard liquid for initial contact angle measurements, helping to determine the hydrophilicity of the membrane surface. Table 5 shows that water contact angles decreased with increasing fullerenol concentration, indicating that membrane surfaces became more hydrophilic due to the increased amount of polar groups thereon. Conversely, membrane surfaces became less hydrophilic at increased heating times due to profound cross-linking between PVA chains and fullerenol that reduced the number of hydroxyl groups, in agreement with the decreased sorption observed at elevated treatment temperatures. Thus, we concluded that addition of fullerenol (even in low amounts) significantly contributed to the increase of surface polarity.

Table 5
Water contact angles measured at 20 °C.

Membranes (heated at 140 °C)	Contact angle (°)		
	100 min	240 min	420 min
PVA	53.6 ± 1.7	58.1 ± 1.5	59.75 ± 1.3
PVA-1% fullerenol	35.0 ± 2.9	38.6 ± 2.6	41.9 ± 1.9
PVA-5% fullerenol	22.2 ± 2.1	25.6 ± 2.2	28.5 ± 1.4

3.6. Pervaporation through dense and supported PVA membranes thermally treated at 140 °C for 100, 240, and 420 min

Initially, supported composite membranes heated for 100 min were prepared, with the effects of 240- and 420-min heating on pervaporation performance further investigated.

The pervaporation characteristics of dense and supported membranes based on pristine PVA thermally cross-linked at 140 °C for 100, 240, and 420 min were tested in the separation of an AcOH/water mixture (10 wt.% water, 90 wt.% AcOH) at 40 °C, with results presented in Table 6.

Table 6

Pervaporation of an AcOH/water mixture (10 wt.% water, 90 wt.% AcOH) at 40 °C through dense and supported PVA membranes.

Heating time	Dense PVA membranes treated at 140 °C			Supported PVA membranes treated at 140 °C		
	Flux (kg/(m ² h))	Water content in permeate (wt.%)	PSI (kg/(m ² h))	Flux (kg/(m ² h))	Water content in permeate (wt.%)	PSI (kg/(m ² h))
100 min	0.023	89.6	1.76	0.185	83.5	8.24
240 min	0.012	93.8	1.62	0.133	87.4	8.17
420 min	0.009	98.8	6.66	0.102	92.1	10.60

The obtained data show that heat treatment significantly increased the selectivity of dense and supported PVA membranes (by up to 9%), also increasing the flux through supported membranes 9- to 10-fold. Therefore, comparison of these results with those achieved after basic treatment at 140 °C for 100 min shows that it is possible to increase the flux by a factor of 5–6 while concomitantly increasing pervaporation selectivity by up to 3%.

Thus, based on pervaporation experiment results and PSI factors, optimal thermal cross-linking conditions were shown to correspond to 140 °C and 420 min, achieving highly selective separation of the AcOH/water mixture.

3.7. Pervaporation through supported membranes based on PVA and PVA-fullerenol composites thermally treated at 140 °C for 420 min

Tables 2 and 3 demonstrate that the introduction of fullereneol increases selectivity by promoting cross-linking. Therefore, to further improve the selectivity of supported membranes, we studied the transport properties of thermally cross-linked supported membranes based on PVA-fullerenol (1 and 5 wt.% with respect to polymer) annealed at 140 °C for 420 min, with results shown in Table 7.

The data in Table 7 show once more that fullereneol incorporation increases pervaporation selectivity, slightly decreasing the flux (by 10%) due to cross-linking of PVA polymer chains and increasing the PSI factor 1.78-fold (to 18.71 kg/(m² h)). Hence, it can be concluded that the best combination of transport properties was obtained for the PVA-5-420^{sup} membrane. However, to further evaluate the application potential of this supported membrane for acetic acid dehydration, additional experiments were carried out, taking into account the variation of feed temperature and feed water content.

3.8. Effect of operating parameters on the transport properties of PVA-5-420^{sup}

Two parameters were investigated to study the transport properties of the above novel composite membrane to evaluate its potential applications in an industrial process. The influence of feed temperature (25, 40, 50, 60 °C) was analyzed because industrial processes benefit from low-temperature operation due to using waste heat streams, and separation of AcOH/water feed mixtures was performed for a wide range of water contents (up to 30 wt.%) to evaluate membrane stability at relatively high water levels.

Table 7

Pervaporation of an AcOH/water mixture (10 wt.% water, 90 wt.% AcOH) at 40 °C through supported membranes based on PVA and PVA-fullerenol composites.

Supported membranes (140 °C, 420 min)	Flux (kg/(m ² h))	Water content in permeate (wt.%)	PSI (kg/(m ² h))
PVA-420 ^{sup}	0.102	92.1	10.60
PVA-1-420 ^{sup}	0.095	93.2	11.62
PVA-5-420 ^{sup}	0.087	96.0	18.71

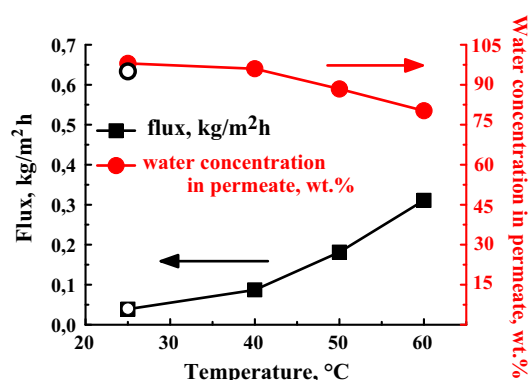


Fig. 7. Dependence of water flux (black curve) and concentration in the permeate (red curve) on temperature during the pervaporation of a water/AcOH mixture through the PVA-5-420^{sup} membrane. Open symbols show membrane parameters determined after completing this set of experiments at the initial temperature of 25 °C to evaluate membrane resistance after exposure to high temperature.

3.8.1. Effect of temperature on the transport properties of PVA-5-420^{sup}

Pervaporation experiments for the separation of a water/AcOH mixture (10/90 w/w) at different temperatures (25, 40, 50, and 60 °C) were performed to determine membrane stability, with the effect of temperature on flux and selectivity shown in Fig. 7.

Fig. 7 shows that the flux through the PVA-5-420^{sup} membrane increased with increasing temperature, as expected, with the permeate water content decreasing to 80 wt.% above 40 °C. After completing experiments at 60 °C, the system was returned to 25 °C to check for hysteresis effects. As a result, the membrane still exhibited high selectivity (98 wt.% water in the permeate, flux = 0.04 kg/(m² h)), showing well-reproducible performance and suitability for continuous operation at several temperatures.

3.8.2. Effect of feed water content on the transport properties of PVA-5-420^{sup}

To assess the opportunities and prospects of applying the abovementioned PVA composite membrane in a real industrial hybrid process successively combining distillation and pervaporation steps [3], its stability was investigated at high feed water contents. The mixture exiting the distillation column may have a water content above 10 wt.%, requiring the membrane to be stable under such conditions. Thus, the transport properties of PVA-5-420^{sup} were investigated for AcOH/water mixtures containing up to 30 wt.% of water.

Finally, the results obtained for PVA-5-420^{sup} were compared to the pervaporation properties of a commercially available membrane, i.e., PERVAPTM 1201 provided by Sulzer, known for its good dehydrating performances in acidic media. The results of this comparative analysis are shown in Figs. 8 and 9.

At low water contents, both membranes exhibited high permeate enrichment (>95 wt.%) (Fig. 8). At higher feed water content, the selectivity of the PVA-5-420^{sup} membrane decreased (85 wt.% water in permeate), whereas that of the PERVAPTM 1201 membrane remained unchanged (~99 wt.% water in permeate).

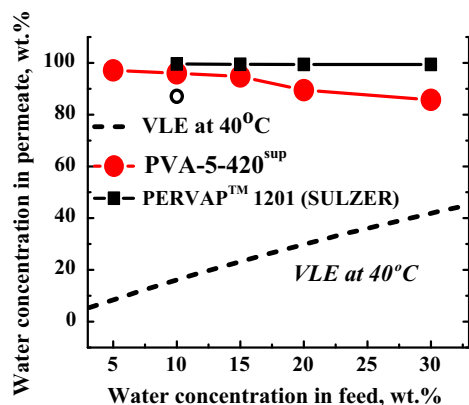


Fig. 8. Dependence of the water content of the permeate on the feed during the pervaporation of a water/AcOH mixture through PVA-5-420^{sup} and PERVAPTM 1201 membranes at 40 °C. Filled symbols denote membrane parameters determined during the experiment as the feed water content was increased from 5 to 30 wt.%. The open symbol shows membrane parameters determined after this set of experiments for the initial water/AcOH mixture (10/90 w/w) to evaluate membrane resistance to high water levels. Vapor-liquid equilibrium data was taken from [2].

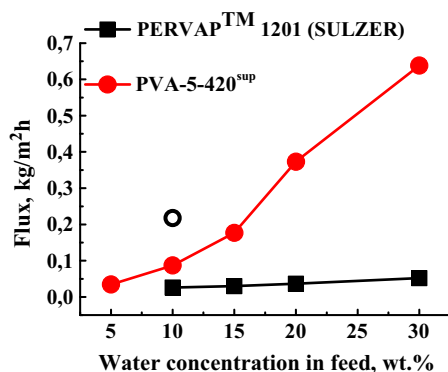


Fig. 9. Dependence of flux on the feed water content during the pervaporation of a water-AcOH mixture through PVA-5-420^{sup} and PERVAP 1201 membranes at 40 °C. Filled symbols denote membrane parameters determined during the experiment as the water content of the feed was increased from 5 to 30 wt.%. The open symbol shows membrane parameters determined after this set of experiments for the initial water/AcOH mixture (10/90 w/w) to evaluate membrane resistance to high water levels.

In both cases, the water content curves significantly differed from the vapor-liquid equilibrium curve (dashed line) of the water-AcOH system (Fig. 8), indicating the high selectivity of these membranes for concentrated acid dehydration.

The data presented in Fig. 9 show that the PERVAP 1201 membrane exhibited a low flux irrespective of the feed water content. Conversely, the flux through the developed PVA membrane containing 5 wt.% fullereneol always exceeded that through the PERVAP membrane, significantly increasing with increasing feed water content (up to 10-fold).

To evaluate membrane resistance to high water levels, pervaporation experiments with PVA-5-420^{sup} were carried out again at a low feed water content (10 wt.% water), revealing that the dehydration performance of this membrane was still very high and achieving permeate enrichment of up to 92 wt.% water, with the corresponding flux increasing to 0.2 kg/(m² h) (initially, 96 wt.% water in the permeate and a flux of 0.08 kg/(m² h) were obtained). This hysteresis effect could be caused by significant membrane swelling in the previous experiment, resulting in a more plasticized polymer matrix.

However, it should be emphasized that despite the slight reduction of membrane selectivity, the transport properties of

PVA-5-420^{sup} remained at a very high level, especially for concentrated acidic mixtures. Hence, this membrane showed stability and high selectivity for the dehydration of acetic acid, exhibiting superior performance compared to that of the commercially available PERVAPTM 1201 membrane.

4. Conclusions

Novel and thermally cross-linked PVA-based supported membranes containing up to 5 wt.% C₆₀(OH)₁₂ were prepared, featuring dense selective layers of ~1.5 μm thickness to achieve high membrane permeance and high selectivity for water.

This study provides two types of very interesting results directly linked to fullereneol nanoparticles introduced at controlled low amounts. The first set of results is related to the physical properties of the modified PVA mixed matrices:

- the polymer matrix is highly crystalline, as shown by XRD analysis;
- the surface polarity is significantly increased by modification with fullereneol, as revealed by the decreased contact angle; and
- the high degree of cross-linking results in low water sorption and high stability in acidic medium.

The second set of results is related to the improved pervaporation performances of the PVA mixed-matrix membrane series:

- PVA-fullereneol nanocomposite prepared in water allow the preparation of supported PVA membranes with a thin dense layer (about 1.5 μm thick) exempt from defects, resulting in high selectivity and high permeances;
- the relationship between flux and selectivity can be very well controlled by choosing appropriate thermal treatment conditions; and
- high stability in concentrated acetic acid mixtures makes these membranes promising candidates for potential industrial application.

These results are clearly linked to the homogeneous distribution of fullereneol nanoparticles in the PVA matrix and the low level of their aggregation, which allow defect-free supported membranes with excellent dehydrating properties to be prepared.

Acknowledgment

This work was supported by Fellowship of the President of Russia [CII-1153.2015.1], Russian Foundation for Basic Research [grant no. 15-58-04034], St. Petersburg State University [No. 12.42.715.2017, 12.42.716.2017], Program UMNIC [No. 106601Y2/2015], the Government of the Russian Federation [grant 074-U01], the financial support from Région Lorraine, France [ARCUS 3 program]. The experimental work of this study was facilitated by equipment from the Resource Centers of GEOMODEL, Center for X-ray Diffraction Methods, the Chemical Analysis and Materials Research Centre, and the Interdisciplinary Resource Center for Nano Technology at St. Petersburg State University.

References

- [1] S.K. Ogorodnikov, T.M. Lesteva, V.B. Kogan, Azeotropic mixtures, Chemistry, St. Petersburg, 1971.
- [2] V.B. Kogan, V.M. Fridman, V.V. Kafarov, *The Equilibrium between Liquid and Vapor*, 1st ed., The science, Moscow-Leningrad, 1966.
- [3] C. Serval, D. Roizard, E. Favre, D. Horbez, Improved energy efficiency of a hybrid pervaporation/distillation process for acetic acid production: identification of target membrane performances by simulation, *Ind. Eng. Chem. Res.* 53 (2014) 7768–7779. <http://dx.doi.org/10.1021/ie500467k>.

- [4] Q. Kang, J. Huybrechts, B. Van Der Bruggen, J. Baeyens, T. Tan, R. Dewil, Hydrophilic membranes to replace molecular sieves in dewatering the bio-ethanol/water azeotropic mixture, *Sep. Purif. Technol.* 136 (2014) 144–149, <http://dx.doi.org/10.1016/j.seppur.2014.09.009>.
- [5] Zion Market Research, Acetic Acid Market for VAM, Acetate Esters, Acetic Anhydride, PTA and Other Application: Global Industry Perspective, Comprehensive Analysis and Forecast, 2015 - 2021, 2016.
- [6] S.K. Ray, S.B. Sawant, J.B. Joshi, V.G. Pangarkar, Dehydration of acetic acid by pervaporation, *J. Memb. Sci.* 138 (1998) 1–17, [http://dx.doi.org/10.1016/S0376-7388\(97\)00210-X](http://dx.doi.org/10.1016/S0376-7388(97)00210-X).
- [7] N. Durmaz-Hilmioglu, A.E. Yildirim, A.S. Sakaoglu, S. Tulbentci, Acetic acid dehydration by pervaporation, *Chem. Eng. Process. Process Intensif.* 40 (2001) 263–267, [http://dx.doi.org/10.1016/S0255-2701\(00\)00122-7](http://dx.doi.org/10.1016/S0255-2701(00)00122-7).
- [8] K.S.V. Krishna Rao, B. Vijaya Kumar Naidu, M.C.S. Subha, M. Sairam, N.N. Mallikarjuna, T.M. Aminabahi, Novel carbohydrate polymeric blend membranes in pervaporation dehydration of acetic acid, *Carbohydr. Polym.* 66 (2006) 345–351, <http://dx.doi.org/10.1016/j.carbpol.2006.03.024>.
- [9] N. Jullok, T. Deforche, P. Luis, B. Van der Bruggen, Sorption and diffusivity study of acetic acid and water in polymeric membranes, *Chem. Eng. Sci.* 78 (2012) 14–20, <http://dx.doi.org/10.1016/j.ces.2012.04.022>.
- [10] R.Y.M. Huang, A. Moreira, R. Notarfonzo, Y.F. Xu, Pervaporation separation of acetic acid-water mixtures using modified membranes. I. Blended polyacrylic acid (PAA)-nylon 6 membranes, *J. Appl. Polym. Sci.* 35 (1988) 1191–1200, <http://dx.doi.org/10.1002/app.1988.070350506>.
- [11] F.U. Nigiz, H. Dogan, N.D. Hilmioglu, Pervaporation of ethanol/water mixtures using clinoptilolite and 4A filled sodium alginate membranes, *Desalination* 300 (2012) 24–31, <http://dx.doi.org/10.1016/j.desal.2012.05.036>.
- [12] X.-S. Wang, Q.-F. An, Q. Zhao, K.-R. Lee, J.-W. Qian, C.-J. Gao, Preparation and pervaporation characteristics of novel polyelectrolyte complex membranes containing dual anionic groups, *J. Memb. Sci.* 415 (2012) 145–152, <http://dx.doi.org/10.1016/j.memsci.2012.04.045>.
- [13] W. Zhang, X. Zhao, Z. Zhang, Y. Xu, X. Wang, Preparation of poly(vinyl alcohol)-based membranes with controllable surface composition and bulk structures and their pervaporation performance, *J. Memb. Sci.* 415 (2012) 504–512, <http://dx.doi.org/10.1016/j.memsci.2012.05.037>.
- [14] M. Mulder, BASIC PRINCIPLES OF MEMBRANE TECHNOLOGY, Moscow, 1999.
- [15] H.M. van Veen, M.M.A. van Tue, Y.C. van Delft, E.R. van Selow, A. x de Groot, Acetic acid dehydration using HybSi[®]-AR membranes, *Energy Res. Cent.* (2016).
- [16] P.D. Chapman, T. Oliveira, A.G. Livingston, K. Li, Membranes for the dehydration of solvents by pervaporation, *J. Memb. Sci.* 318 (2008) 5–37, <http://dx.doi.org/10.1016/j.memsci.2008.02.061>.
- [17] W. Zhang, Y. Xu, Z. Yu, S. Lu, X. Wang, Separation of acetic acid/water mixtures by pervaporation with composite membranes of sodium alginate active layer and microporous polypropylene substrate, *J. Memb. Sci.* 451 (2014) 135–147, <http://dx.doi.org/10.1016/j.memsci.2013.09.027>.
- [18] N. Jullok, R. Van Hooghten, P. Luis, A. Volodin, C. Van Haesendonck, J. Vermant, et al., Effect of silica nanoparticles in mixed matrix membranes for pervaporation dehydration of acetic acid aqueous solution: plant-inspired dewatering systems, *J. Clean. Prod.* 112 (2016) 4879–4889, <http://dx.doi.org/10.1016/j.jclepro.2015.09.019>.
- [19] J.H. Chen, J.Z. Zheng, Q.L. Liu, H.X. Guo, W. Weng, S.X. Li, Pervaporation dehydration of acetic acid using polyelectrolytes complex (PEC)/11-phosphotungstic acid hydrate (PW11) hybrid membrane (PEC/PW11), *J. Memb. Sci.* 429 (2013) 206–213, <http://dx.doi.org/10.1016/j.memsci.2012.11.038>.
- [20] M.H. Zhu, I. Kumakiri, K. Tanaka, H. Kita, Dehydration of acetic acid and esterification product by acid-stable ZSM-5 membrane, *Micropor. Mesopor. Mater.* 181 (2013) 47–53, <http://dx.doi.org/10.1016/j.micromeso.2012.12.044>.
- [21] A.V. Penkova, S.F.A. Acquah, M.E. Dmitrenko, B. Chen, K.N. Semenov, H.W. Kroto, Transport properties of cross-linked fullereneol-PVA membranes, *Carbon N. Y.* 76 (2014) 446–450, <http://dx.doi.org/10.1016/j.carbon.2014.04.053>.
- [22] A.V. Penkova, S.F.A. Acquah, M.P. Sokolova, M.E. Dmitrenko, A.M. Toikka, Polyvinyl alcohol membranes modified by low-hydroxylated fullereneol C60 (OH)₁₂, *J. Memb. Sci.* 491 (2015) 22–27, <http://dx.doi.org/10.1016/j.memsci.2015.05.011>.
- [23] A.V. Penkova, S.F.A. Acquah, M.E. Dmitrenko, M.P. Sokolova, M.E. Mikhailova, E. S. Polyakov, et al., Improvement of pervaporation PVA membranes by the controlled incorporation of fullereneol nanoparticles, *Mater. Des.* 96 (2016) 416–423, <http://dx.doi.org/10.1016/j.matdes.2016.02.046>.
- [24] A.C. Larson, General Structure Analysis System (GSAS), Los Alamos Lab. Rep. 748 (1994) 86–748, <http://dx.doi.org/10.1103/PhysRevLett.101.107006>.
- [25] B.H. Toby, EXPGUI, a graphical user interface for GSAS, *J. Appl. Crystallogr.* 34 (2001) 210–213, <http://dx.doi.org/10.1107/S0021889801002242>.
- [26] J.K. Kujawski, W.M. Kujawski, H. Sondej, K. Jarzynka, A. Kujawska, M. Bryjak, et al., Dewatering of 2,2,3,3-tetrafluoropropan-1-ol by hydrophilic pervaporation with poly(vinyl alcohol) based Pervap[™] membranes, *Sep. Purif. Technol.* 174 (2017) 520–528, <http://dx.doi.org/10.1016/j.seppur.2016.10.041>.
- [27] C.W. Bunn, Crystal structure of polyvinyl alcohol, *Nature* 161 (1948) 929–930, <http://dx.doi.org/10.1038/161929a0>.
- [28] J.D. Cho, W.S. Lyoo, S.N. Chvalun, J. Blackwell, X-ray Analysis and Molecular Modeling of Poly(vinyl alcohol)s with Different Stereoregularities, 1999. 10.1021/MA9908402.
- [29] W.A. Dollase, Correction of intensities for preferred orientation in powder diffractometry: application of the March model, *J. Appl. Crystallogr.* 19 (1986) 267–272, <http://dx.doi.org/10.1107/S0021889886089458>.
- [30] M. Wojdyr, Fityk: a general-purpose peak fitting program, *J. Appl. Crystallogr.* 43 (2010) 1126–1128, <http://dx.doi.org/10.1107/S0021889810030499>.